Electronic Supplementary Material (ESI) for Nanoscale.

Supporting Information

Quantitative Description of Thermodynamic and Kinetic Properties of the Platelet factor 4/Heparin Bonds

Thi-Huong Nguyen,[*a] Andreas Greinacher,[b] and Mihaela Delcea[*a]

[*]E-mail: thihuong.nguyen@uni-greifswald.de; delceam@uni-greifswald.de

For tip functionalization, we compared the adhesion forces among bare tip (Fig. S1a), PEG-NH_2 coated tip (Fig. S1b), and heparin linked to PEG-NH_2 coated tip against gold surface (Fig. S1c). The adhesion forces are completely different either from shape of retraction curves or magnitude of adhesion forces depending on their surface chemistry. For bare tip, we obtained large adhesion forces, but the retraction parts of F-D curves did not show non-linear behavior (Fig. S1a), indicating stretching of polymer. For the PEG-NH_2 coated tip (Fig. S1b), we obtained very small adhesion forces. The adhesion forces increased significantly when the heparin was linked to PEG-NH_2 tip (Fig. S1c). To neglect the interactions between heparin/tip and free PEG-COOH linkers (which do not bind PF4 on the substrate), we measured the adhesion forces of this pairs. Only few rupture events in 1000 measurements were observed (Fig. S1d). When we measured the interaction between PF4 immobilized on the tip and PF4 immobilized on substrate, we found a strong electrostatic repulsive force (ER) (Fig. S1e).

For surface modification, we also ensured that PF4 was immobilized on the substrate by comparing the adhesion force between bare tip and gold surface (Fig. S1a), PEG-COOH coated gold surface (Fig. S1f), and PF4 coated PEG-COOH surface (Fig. S1g). Small adhesion forces were measured between bare tip and PEG-COOH coated gold surface (Fig. S1f), but large variation of rupture forces and different shapes of F-D curves were observed from measurements of bare tip against PF4 coated surface (Fig. S1g). To ensure that the interactions between PEG-NH_2 on the tip and PF4 on the substrate do not influence our heparin/PF4 interaction measurement, we measured the adhesion forces of this pair and found that only few adhesive events in 1000 measurements were obtained (Fig. S1h).

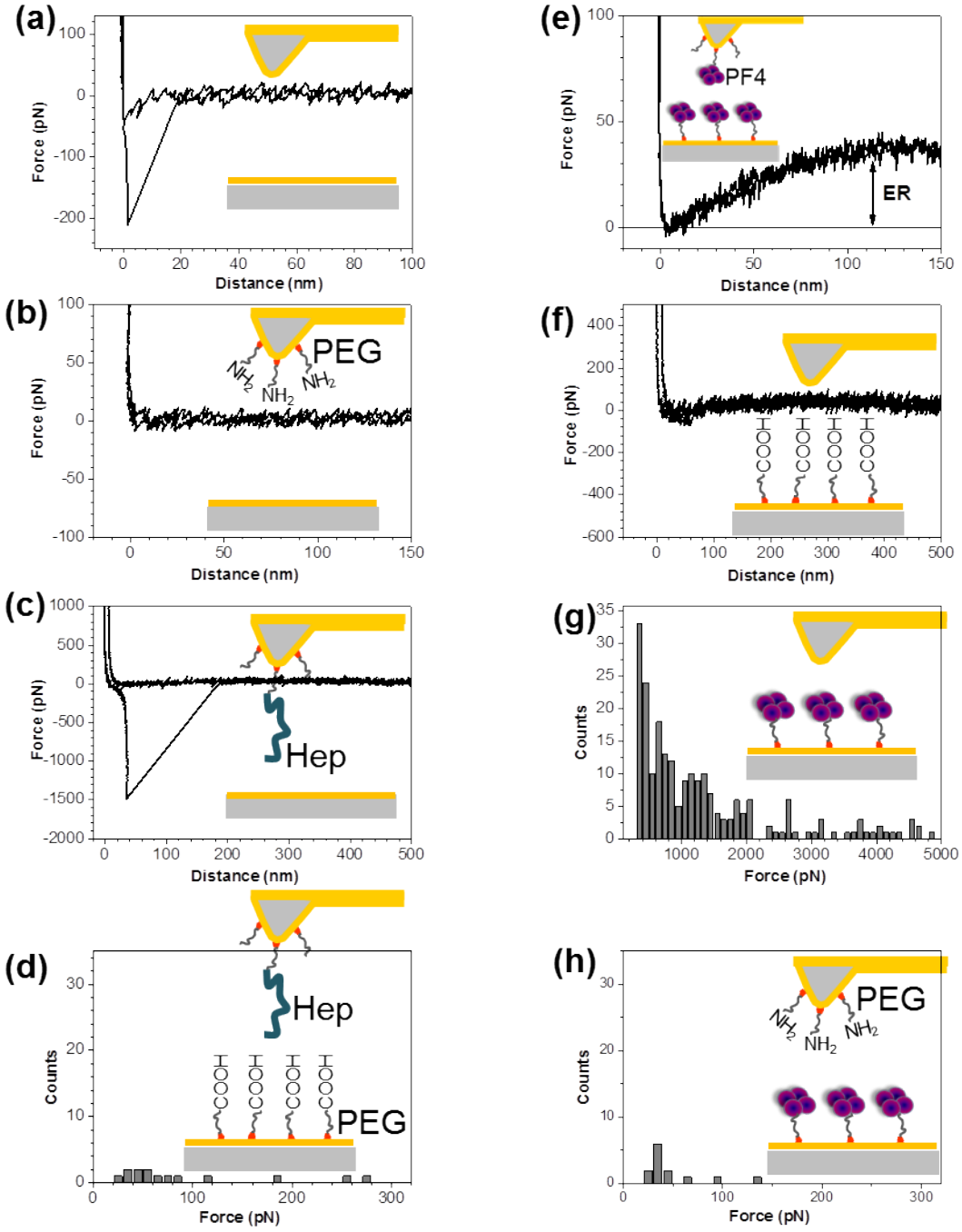

Figure S1. Control experiments for tip and substrate functionalization. (a) A bare AFM tip interacts with a gold-coated substrate showing a retraction curve without polymer stretching behavior. (b) PEG-NH_2 coated tip does not show any adhesion with the bare gold surface. (c) After linking heparin to the PEG-NH_2 coated tip, a large adhesion force is recorded. (d) Heparin does not interact with PEG-COOH coated surface which is used to link PF4 to the substrate (only few adhesion events were obtained among 1000 F-D curves). (e) PF4-PF4 interaction exhibits a strong electrostatic repulsive force (ER). (f) Bare tip interacts weakly with PEG-COOH coated surface. (g) Bare tip adheres to PF4 tetramers strongly showing a large range of rupture forces. (h) PEG-NH_2 coated tip does not interact with PF4.

We confirmed the immobilization of PF4 on gold surface by comparing AFM images among three surfaces, *i.e.,* the bare gold surface (Au), the surface coated with PEG-COOH (PEG/Au), and PEG/Au surface coated with PF4 (Fig. S2a). The roughness of gold surface was found to be similar to that of PEG/Au (~ 0.7 nm) while the surface roughness of PEG/Au reduced after coating with PF4 (~0.3 nm) (Fig. S2b).

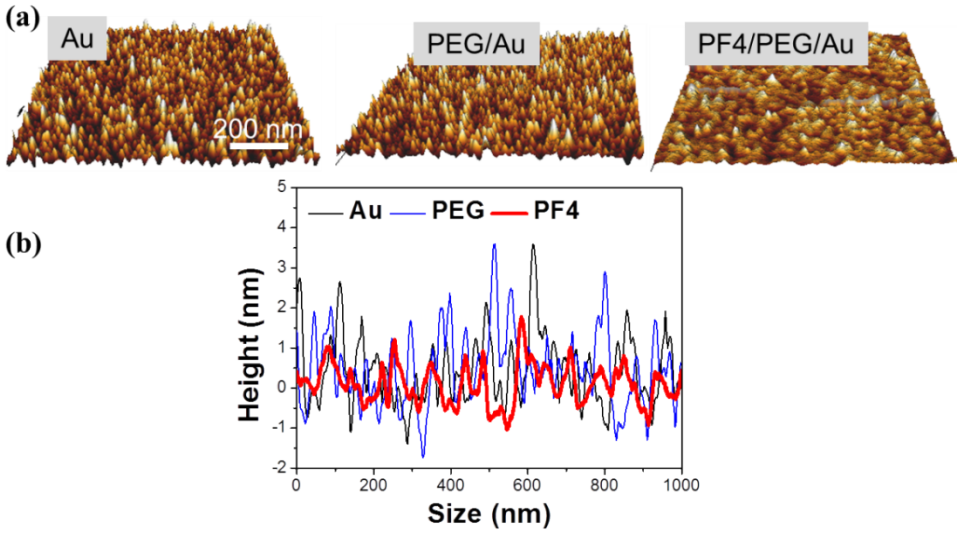

Figure S2. (a) AFM images of gold surface (left), PEG-coated gold surface (middle) and PF4-coated PEG/gold surface (right). (b) The roughness of gold surface (black) does not change significantly after coating with PEG (blue), but reduces after coating with PF4 (red).

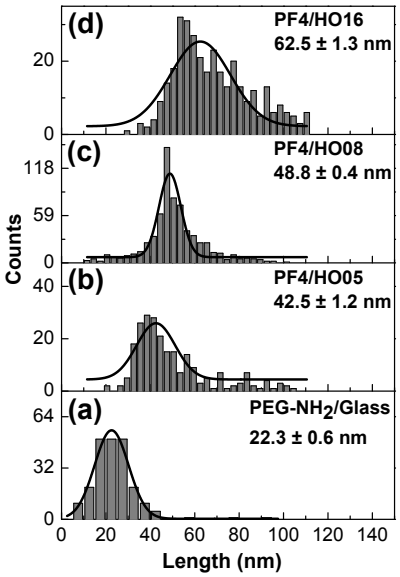

Figure S3. Selected probability distributions of the rupture distances from F-D curve measurements for PEG-NH_2/Glass (a), HO05 (b), HO08 (c), and HO16 (d). PEG linker is stretched during the interaction with the glass surface, resulting in a contour length of about 22 nm. Three-fold increase in the contour length for the PF4/HO05 and PF4/HO08 is due to the stretching of both PEG on the tip (for attachment of heparin) and PEG on the substrate (for immobilization of PF4). The difference in rupture lengths among these heparins supports the successful immobilization of heparins on the tip. At higher rupture force, we observed higher stretching of the involved linkers (PEG and heparin).

Binding affinity of antibodies to PF4/heparins complexes. Complexes of PF4 with heparins are non-covalently immobilized on plates (Fig. S4a). Purified antibodies or serum containing anti-PF4/heparin antibodies bind to PF4/heparin coated plates (Fig. S4b) and secondary antibodies (goat anti-human antibody) bind to anti-PF4/heparin antibodies (Fig. S4c). An enzyme is introduced to the secondary antibody to amplify and visualize the read-out signal. The more anti-PF4/heparin antibodies bind to PF4/heparin complexes, the higher the fluorescence intensity will be observed. The basic principle of an EIA is that only the specific antibodies bind to their antigen, while all non-bound antibodies are washed away. This makes EIAs the standard tool to detect antibodies with a defined specificity in a mixture of antibodies.

Antibody purification. Anti-PF4/heparin antibodies were separated from patients' sera by affinity chromatography. Complexes of 0.5 U/ml UFH and 20 µg/ml biotinylated PF4 (bPF4) and 20 µg/ml PF4 (30% bPF4:70% PF4) were formed in a buffer solution (50 mM NaH_2PO_4, 65 mM NaN_3, pH 7.5) at RT for 1h. 5 ml streptavidin-coated sepharose beads (GE Healthcare Europe GmbH, Freiburg, Germany) were washed three times with PBS at 5 ^oC, 600 g for 5 min before coating with bPF4/PF4/heparin complexes. The reaction between bPF4 in the bPF4/PF4/heparin complex and streptavidin-coated bead was carried out by mixing the complexes with the beads for 30 min at RT and incubating them at 4 ^oC overnight. Patient's sera was diluted in a buffer solution (50 mM NaH_2PO_4, 150 mM NaCl, pH 7.5) (1:50) and transferred to the bPF4/PF4/heparin coated beads and stirred for 1h at RT before loading to a MidiTrap column (GE Healthcare Limited, Amersham Place, Little Chalfont, Buckinghamshire, HP7 9NA, UK). The sample column was then washed with 8 columns of buffer (150 mM NaCl, 0.1% Tween20, pH 7.5) to remove unbound molecules. After washing, the bound antibodies were eluted by incubating in 0.1 M Glycine buffer, pH 2.7 for 10 min at RT. The collected fractions were neutralized by mixing with Tris buffer pH 9.0. Characteristics of the purified anti-PF4/heparin antibodies were finally checked by enzyme-linked immunosorbent assay, SDS-PAGE, and heparin-induced platelet aggregation test (data not shown) to reconfirm binding, purity, and platelet activating capacity.

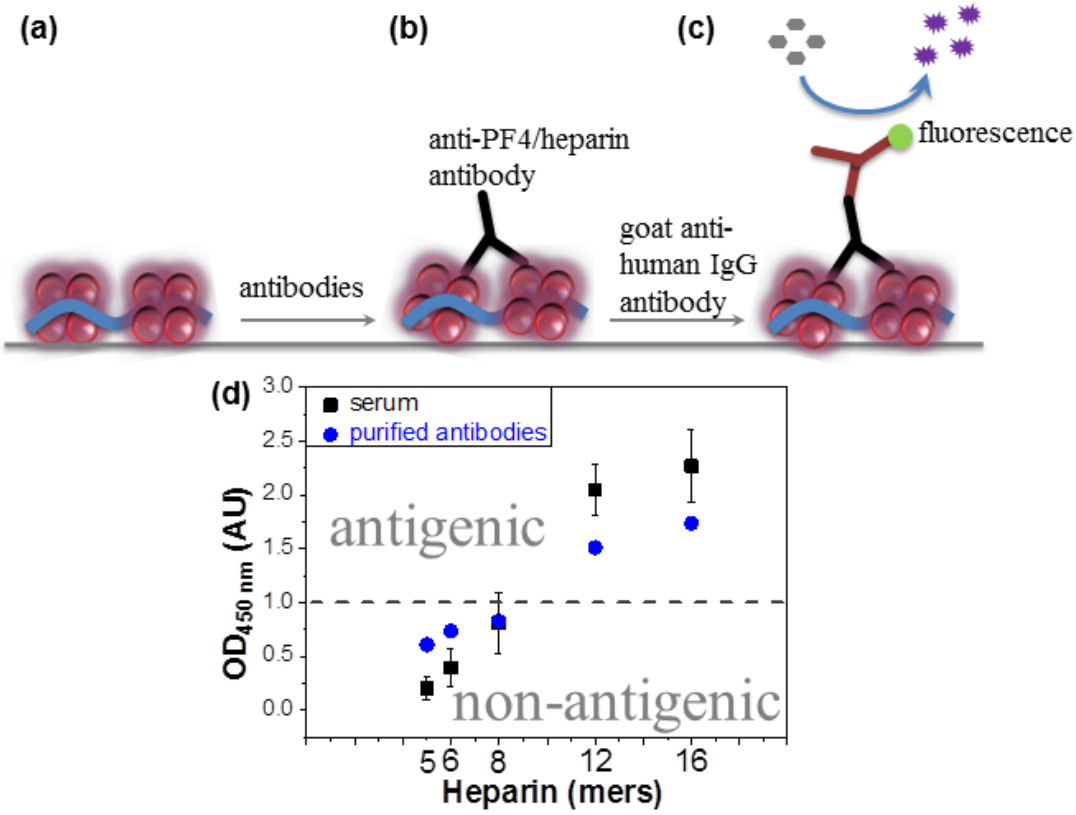

Figure S4. EIA measurements for anti-PF4/heparin antibody binding to PF4/heparin complexes. Substrate coated with PF4/heparin complexes (a) is incubated with anti-PF4/heparin antibodies which bind to PF4 tetramers (b) and the fluorescence from a secondary goat anti-human IgG antibody bound to the anti-PF4/heparin antibody (c), is quantified by the change in OD (d). The black filled squares represent average OD values from sera (error bars corresponding to the standard deviation of three different sera) and the blue filled circles represent OD values from purified antibodies.

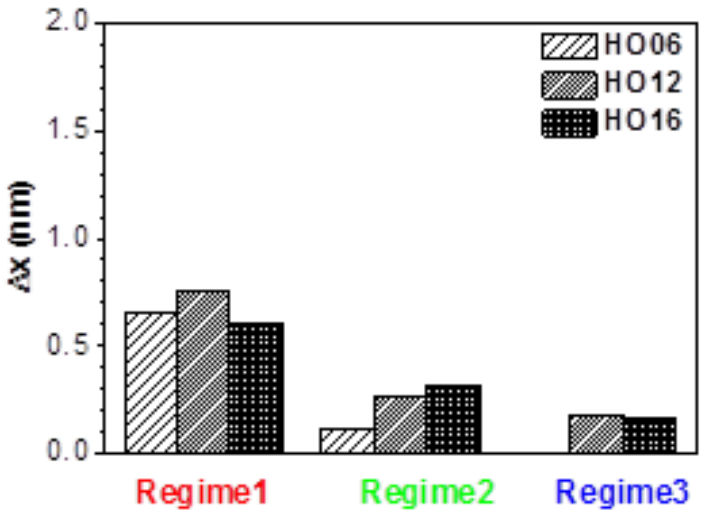

Figure S5. Bond distances (Δx) of PF4/heparin complexes at three different loading rate regimes. Bond distance reduces from regime 1 to regime 3.